International Journal of Pharmaceutics 434 (2012) 140–147

Contents lists available at SciVerse ScienceDirect

International Journal of Pharmaceutics

journal homepage: www.elsevier.com/locate/ijpharm

Pharmaceutical Nanotechnology

Influence of choroidal neovascularization and biodegradable polymeric particle size on transscleral sustained delivery of triamcinolone acetonide

Rajendra S. Kadam[a,1], Puneet Tyagi[a,1], Henry F. Edelhauser[b], Uday B. Kompella[a,*]

[a] Departments of Pharmaceutical Sciences and Ophthalmology, University of Colorado Anschutz Medical Campus, Aurora, CO, United States
[b] Emory Eye Center, Emory University, Atlanta, GA, United States

ARTICLE INFO

Article history:
Received 16 December 2011
Received in revised form 19 April 2012
Accepted 15 May 2012
Available online 23 May 2012

Keywords:
Microparticles
Nanoparticles
Triamcinolone acetonide
Choroidal neovascularization

ABSTRACT

Purpose: One objective of this study was to determine whether polymeric nanoparticles and/or microparticles sustain transscleral choroidal and retinal delivery of triamcinolone acetonide (TA) for two months in therapeutically effective concentrations after single periocular administration. Another objective of this study was to assess the influence of choroidal neovascularization on transscleral delivery of TA.
Methods: Polymeric nano- and micro-particles of TA were prepared by o/w emulsion-solvent evaporation method using poly-L-lactide (PLA). Particles were characterized for drug loading, size, surface morphology, and the in vitro drug release profile. Choroidal neovascularization (CNV) was induced in brown Norway (BN) rats using a 532 nm diode argon laser and the CNV induction was assessed using fluorescein angiography. In vivo delivery was assessed in control and CNV induced rats at 2 months after periocular injection of TA loaded nano- or micro-particle suspension, or plain TA suspension in PBS (pH 7.4). Ocular tissue levels of TA were estimated using LC–MS/MS following liquid–liquid extraction of drug from tissue samples. Nile red loaded microparticles entrapped in periocular tissue at the end of the study was visualized using scanning electron microscopy and confocal microscopy. Inhibitory effect of TA on VEGF secretion was evaluated in ARPE-19 cells.
Results: Triamcinolone acetonide-PLA nano- (551 nm) and micro-particles (2090 nm), with 14.7 and 29.5% drug loading, respectively, sustained in vitro TA release for about 45 and 120 days. After subconjunctival injection, microparticles were able to sustain the delivery in all intraocular tissues for 2 months; whereas no drug levels were detected for TA loaded nanoparticles and plain suspension of TA. Intraocular delivery of TA from microparticles was higher in CNV induced rats when compared to control rats. Significant amount of microparticles remained in periocular tissue at 2 months afterinjection, and maintained spherical shape. TA decreased VEGF secretion by 50% at 0.07 μM. At the end of the in vivo study, choroid-RPE and retina TA levels in CNV induced rats were 16- and 5-fold higher than the IC_{50} for VEGF secretion.
Conclusions: Single periocular injection of polymeric microparticles but not nanoparticles sustained effective levels of TA in choroid-RPE and retina for 2 months, with the TA delivery being greater in CNV induced rats than the control rats.

1. Introduction

Age related macular degeneration (AMD) is a leading cause of blindness amongst the elderly population. In the United States alone, more than 8 million people suffer from the AMD and this number is expected to increase by 50% by 2020 (Jager et al., 2008). AMD is a chronic, multifactorial, life-long ocular disease. Available medical treatment helps to avoid further progression of the disease, but cannot cure the disease and hence, chronic administration of pharmaceutical therapy is necessary (Nowak, 2006). Current gold standard for the treatment of the wet or neovascular form of AMD is ranibizumab, an antibody fragment that binds vascular endothelial growth factor (VEGF). Further, bevacizumab, a full length VEGF antibody and triamcinolone acetonide (TA), a corticosteroid, are being used off-label to treat wet AMD (Nowak and Bienias, 2007).

In AMD, therapeutic agents need to reach the retina and choroid-retinal pigmented epithelium (RPE) to exert their action.

* Corresponding author at: Department of Pharmaceutical Sciences, University of Colorado Anschutz Medical Campus, 12850 E. Montview Blvd., Aurora, CO 80045, United States. Tel.: +1 303 724 4028; fax: +1 303 724 4666.
E-mail address: uday.kompella@ucdenver.edu (U.B. Kompella).
[1] These authors contributed equally to this work.

0378-5173/$ – see front matter © 2012 Elsevier B.V. All rights reserved.
http://dx.doi.org/10.1016/j.ijpharm.2012.05.025

Drug delivery to the posterior ocular tissues by conventional topical or systemic routes is limited by extraocular epithelial barriers (conjunctival and corneal epithelium) and the blood–tissue barriers (Sunkara and Kompella, 2003). Drug delivery to the posterior segment of the eye is most efficiently achieved by local, ocular routes of administration including intravitreal, subretinal, suprachoroidal, and periocular injections (Raghava et al., 2004). However, intravitreal and subretinal routes are highly invasive to the retina and repeated injections have a high risk of serious complications including retinal detachment and endophthalmitis (Shah et al., 2011). On the other hand, periocular injections, which include subconjunctival, subtenon, peribulbar, retrobulbar, and posterior juxtascleral injections, are generally considered safer, as these are more peripheral to the eye (Raghava et al., 2004).

Triamcinolone acetonide is the most commonly used off-label steroid treatment for AMD and vitreoretinal disorders (Jonas et al., 2002). Vitreal half-life of TA after intravitreal injection of 0.3 mg drug suspension in vitrectomized and nonvitrectomized rabbits is 1.57 days and 2.89 days, respectively (Chin et al., 2005). In order to maintain the effective concentration of TA in the target tissue for prolonged periods, the patient must be administered a high initial dose or receive frequent injections. Higher intravitreal concentration of TA is associated with various side effects including blurred vision, cataract, elevated intraocular pressure, and retinal cell damage (Ozkiris and Erkilic, 2005; Schlichtenbrede et al., 2009). Therefore, the most common approach for achieving therapeutic levels of TA in the target tissue is to administer frequent intravitreal injections, which as described above increases the risk for injection-related complications. An alternative to intravitreal injection is periocular injection of TA, which is a less invasive and a safer option for delivery of TA to the choroid-RPE and retina at effective concentrations. The major problem with periocular injection of TA suspension is the very short half-life of TA in the periocular space because of conjunctival lymphatic and blood clearance (Robinson et al., 2006). Cheruvu et al. showed that the choroid-RPE half-life of celecoxib, a drug that is less soluble than TA, is 3.7 h after subconjunctival injection of celecoxib suspension in Brown Norway rats (BN) (Cheruvu et al., 2008). Similar to intravitreal injection, patients treated with periocular injections must be administered multiple injections in order to maintain effective concentrations, which is inconvenient and costly. Sustained delivery systems can maintain effective drug levels for prolonged periods of time, thereby reducing the dosing frequency (Kompella et al., 2010). Drug encapsulated in biodegradable polymeric nano- and micro-particles with properly designed vehicles are clinically viable options for the sustained delivery of drug molecules administered by periocular injection. A previous report from our laboratory showed the effectiveness of subconjunctivally injected celecoxib-PLGA microparticles for two months in a diabetic retinopathy model (Amrite et al., 2006). Further, the transscleral delivery of therapeutic agents to the posterior ocular tissues can be higher in AMD patients due to compromised ocular barriers and altered clearance. Significant reduction in choroidal blood flow in AMD patients has been previously reported (Grunwald et al., 1998, 2005). Additionally, growth of new choroidal vessels into and through the retinal pigment epithelium (RPE) or subretinal space can result in loss of the RPE barrier integrity (Dobi et al., 1989; Dong et al., 2011), which can lead to enhanced transscleral delivery of therapeutic agents. Previously we observed enhanced delivery of celecoxib to the choroid and retina in a diabetic rat as compared to control rats (Cheruvu et al., 2009). No reports are currently available regarding delivery of therapeutic agents in choroidal neovascularization.

Based on all the above reasoning, the main objective of this study was to determine the influence of choroidal neovascularization (CNV) on transscleral delivery of TA. Another objective of this study was to develop polymeric, biodegradable nano- and micro-particles and assess their ability to sustain TA delivery to choroid-RPE and retina in therapeutically effective concentrations for at least two months.

2. Materials and methods

2.1. Materials

Poly-(L-lactide) (PLA), with inherent viscosity of 0.95–1.20 dL/g (product No. B6002-2P), was purchased from Birmingham Polymers (Pelham, AL). Triamcinolone acetonide was purchased from Spectrum Chemical Mfg. Corp (New Brunswick, NJ). Dichloromethane, poly (vinyl alcohol) of Mw 30,000–70,000, acetonitrile, and sodium azide were purchased from Sigma Aldrich (St. Louis, MO). All other chemicals and reagents used in this study were of analytical reagent grade.

2.2. Preparation of triamcinolone acetonide loaded nanoparticles and microparticles

Nanoparticles were prepared by an o/w emulsion-solvent evaporation method. PLA polymer (200 mg) was dissolved in 5 ml dichloromethane and mixed with 1 ml dichloromethane containing TA (100 mg) and Nile red (0.5 mg). The drug polymer solution was transferred to 30 ml of cold 2% (w/v) aqueous polyvinyl alcohol solution in an ice bath under sonication (Misonix Sonicator 3000, Farmingdale, NY) at 3 W for 2 min to prepare an o/w emulsion. The o/w emulsion was transferred to 100 ml chilled 2% (w/v) aqueous polyvinyl alcohol solution in an ice bath under sonication at 12–15 W for 2 min to stabilize the emulsion. The emulsion was stirred for 3 h at room temperature using a magnetic stirrer to harden the nanoparticles. The hardened nanoparticles were then centrifuged for 20 min at 27,000 × *g* using an ultracentrifuge. The nanoparticle pellet was washed twice with 150 ml of distilled water. The final pellet was dispersed in 10 ml of double distilled water and lyophilized in a Labconco freeze dryer (Labconco Corporation, Kansas City, MO) over 24 h.

TA loaded microparticles were also prepared by o/w emulsion-solvent evaporation method. PLA polymer (200 mg) was dissolved in 5 ml of dichloromethane. TA (100 mg) and 1 ml of Nile red solution (0.5 mg/ml solution in dichloromethane) were dissolved in the above polymer solution. The drug polymer dispersion was transferred to 30 ml of 2% w/v aqueous polyvinyl alcohol solution under homogenization at 10,000 rpm for 2 min using a Virtishear Cyclone® Homogenizer. The above o/w emulsion was further transferred to 100 ml of 2% (w/v) aqueous polyvinyl alcohol solution under homogenization at 10,000 rpm for 5 min using a Virtishear Cyclone® Homogenizer. The final emulsion was stirred for 3 h using a magnetic stirrer. The microparticles thus formed were centrifuged at 10,000 × *g* for 20 min. The microparticle pellet obtained after centrifugation was washed twice with 150 ml of distilled water. The final microparticle pellet was redispersed in 10 ml double distilled water and lyophilized in a Labconco freeze dryer (Labconco Corporation, Kansas City, MO) over 24 h.

2.3. Characterization of nanoparticles and microparticles

Lyophilized particles (1 mg) were resuspended in 5 ml of filtered deionized water to measure particle size and size distribution. Nanosizer (Malvern Inc., Westborough, MA) was used to evaluate particle size and size distribution. Surface morphology was studied with a scanning electron microscope (JSM-6510, Jeol USA, Inc., CA) after mounting particles on aluminum stubs and coating with a layer of gold using a sputter Coater (Anatech USA, CA). TA and Nile red content in the particles was measured by dissolving 1 mg

of lyophilized TA loaded particles in 2 ml chloroform, followed by vortexing (Vortex Genie, Scientific Industries, Bohemia, NY) for 1 h at room temperature. TA and Nile red content was measured in chloroform using UV spectrophotometry (238 nm and 520 nm for TA and Nile red, respectively). Separate standard curves for TA and Nile red were prepared by dissolving a known amount of TA or Nile red in chloroform, followed by serial dilutions. All measurements were done in triplicates. The % drug loading and entrapment efficiency in particles were determined using the following formulas.

$$\text{drug loading (\%)} = \frac{\text{mass of drug in nanoparticles}}{\text{mass of nanoparticles}} \times 100,$$

$$\text{encapsulation efficiency (\%)} = \frac{\text{experimental drug loading}}{\text{theoretical drug loading}} \times 100.$$

2.4. In vitro drug release study

Two milligrams of drug-loaded particles were dispersed in 1 ml of pH 7.4 phosphate buffered saline (PBS). The particle dispersion was transferred into a dialysis membrane bag (7Spectra/por®, Spectrum Laboratories, CA) with a molecular weight cut off of 10,000 Da. The dialysis bag was suspended in 10 ml pH 7.4 PBS containing 0.05% (w/v) sodium azide, maintained at 37 °C in a shaker incubator (Max Q 4000 Shaker, Thermo Scientific, Waltham, MA). Two ml of dissolution medium was withdrawn at various intervals and replaced with drug-free dissolution medium maintained at 37 °C. The amount of drug released in the dissolution medium at each time interval was analyzed by UV spectrophotometer at 238 nm. All incubations were done in triplicates.

2.5. Animals

Animal studies were conducted in accordance with ARVO Statement for the Use of Animals in Ophthalmic and Vision Research and guidelines by animal care committee of University of Colorado Denver. Adult male Brown Norway rats (150–180 g) were purchased from Harlan Sprague Dawley Inc. (Indianapolis, IN, USA).

2.6. Induction and assessment of CNV

Rats were anesthetized using an intraperitoneal injection of 50 mg/kg ketamine and 10 mg/kg xylazine mixture. Pupils were dilated by topical administration of 1% tropicamide solution. A glass cover slip with a drop of 2.5% hypromellose solution was used to visualize the fundus of the rat. Eight laser spots (100 μm, 150 mW, 100 ms) concentric with the optic nerve were placed in the right eye of each rat using a 532 nm diode laser (Oculight Glx; Iridex Inc., Mountain View, CA, USA) and a slit lamp (Zeiss slit lamp 30SL; Carl Zeiss Meditec Inc., Dublin, CA, USA). Left eye was used as a control for each animal. Rats showing hemorrhage upon laser administration were excluded from the study. The Bruch's membrane breakage was confirmed using bubble formation as the end point. CNV lesions were allowed to develop for 14 days after induction of laser burns for tissue distribution studies. Development of CNV was studied using a Fundus camera (Genesis Df, Kowa Optimed, CA) after intravenous injection of 1% sodium fluorescein solution (250 μl) in PBS pH 7.4.

2.7. In vivo tissue distribution

In vivo tissue distribution of TA loaded polymeric nano- or micro-particle dispersions and TA suspension was carried out in normal and CNV induced BN rats. Rats were anesthetized with intraperitoneal injection of 50 mg/kg ketamine and 10 mg/kg xylazine. TA loaded nanoparticle or microparticle dispersion or TA suspension (25 μl containing 150 μg of TA) was administered into the posterior subconjunctival space of right eye (ipsilateral) using a 30-gauge needle ($n = 4$). The left eye was untreated. The animals were allowed to recover from anesthesia, and water and food were provided ad libitum and kept for 2 months. At the end of 2 months, the animals were euthanized by intraperitoneal injection of sodium pentobarbital (250 mg/kg). Eyes and periocular tissues were collected and immediately frozen using a mixture of isopentane and dry ice. Tissues were stored at −80 °C until analysis. Ocular tissues were separated by dissection of the eye in frozen condition on a ceramic tile placed above dry ice isopentane bath. Drug levels were measured in sclera, choroid-RPE, retina, vitreous, lens, cornea, iris-ciliary body, and periocular tissue by an LC–MS/MS method.

2.8. Assessment of nanoparticles and microparticles entrapped in rat periocular tissue

Microparticles entrapped in periocular tissues were visualized using confocal microscopy. For confocal microscopy, tissues were placed on a glass slide and a drop of Supermount mounting medium was added. A cover slip was placed on the tissue and air dried for 2 h before assessment using Nikon C1si® confocal microscope. Confocal microscopy indicated the presence of Nile red dye in periocular tissues. Scanning electron microscopy (SEM) was used to further confirm that particles were present in the tissue. For SEM, tissues were mounted on aluminum stubs and coated with a layer of gold using a sputter Coater (Anatech USA, CA). The morphology was observed with JSM-6510 scanning electron microscope (Jeol USA, Inc., CA) at an accelerating voltage of 5.0 kV.

2.9. VEGF secretion assay

Inhibitory effect of TA on VEGF secretion in ARPE-19 cells was evaluated as per previously described methods (Kompella et al., 2003). Briefly, 4000 cells were seeded per well in a 96-well plate and cultured for 24 h until 70–80% confluency. After 24 h, the culture medium was replaced with serum free medium and cells were allowed to remain in quiescence for 12 h before drug treatment. Cells were treated with 50 nM to 50 μM of TA for 12 h. At the end of 12 h, the medium was collected and the secreted VEGF was quantified using an ELISA kit capable of detecting $VEGF_{165}$ and $VEGF_{121}$ isoforms (Research Diagnostic, Inc., Flanders, NJ).

2.10. Tissue sample processing

TA content in rat ocular tissues was measured after extraction of drugs from tissues by liquid–liquid extraction. Briefly, the weighed amount of ocular tissues were mixed with 500 μl of PBS (pH 7.4) containing 250 ng/mL budesonide (internal standard) in 2 ml microcentrifuge tube, vortexed for 10 min, and then homogenized using a hand homogenizer in an ice bath. Dichloromethane (1.5 ml) was added to this homogenate and vortexed for 10 min using a multitube vortexer (VWR LabShop, Batavia, IL). The organic layer was separated by centrifugation at 10,000 × g for 10 min. Separated organic layer was transferred into clean glass tubes and evaporated under nitrogen stream (Multi-Evap; Organomation, Berlin, MA) at 40 °C. The residue after evaporation was reconstituted with 250 μl of acetonitrile:water (75:25, v/v) and subjected to LC–MS/MS analysis. The liquid–liquid extraction method for extraction of TA from rat ocular tissues was validated to determine the extraction recovery using three different concentrations (low, medium and high) to cover the entire range of expected concentrations of TA in various tissues.

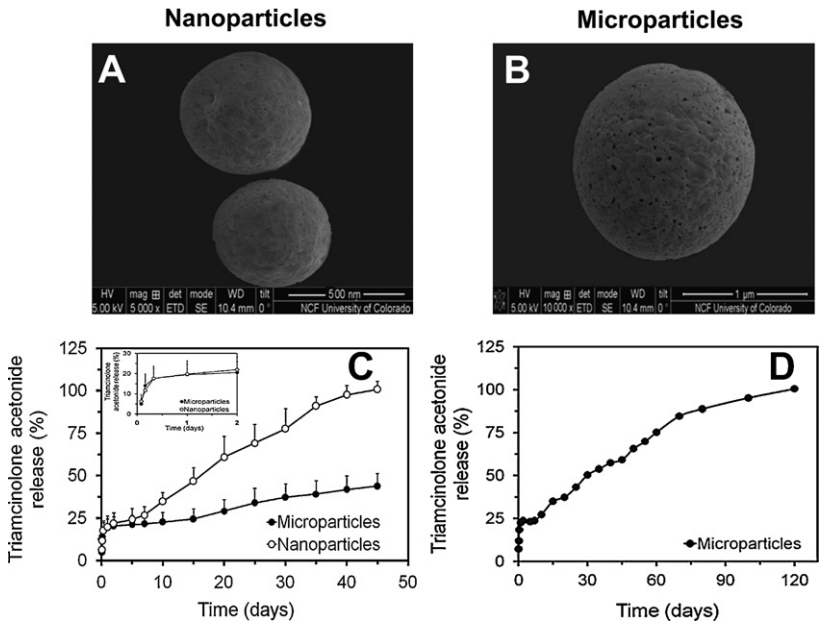

Fig. 1. Size and surface morphology of (A) nanoparticles and (B) microparticles, and (C) in vitro release of triamcinolone acetonide from nanoparticles and microparticles. (D) In vitro release of one sample of microparticles was monitored for 120 days, until complete drug release.

2.11. LC–MS/MS analysis

Ocular tissue levels of TA were measured by means of LC–MS/MS. An API-3000 triple quadrupole mass spectrometer (Applied Biosystems, Foster City, CA, USA) coupled with a PerkinElmer series-200 liquid chromatography (Perkin Elmer, Walthm, Massachusetts, USA) system was used for analysis. Analytes were separated on a Sunfire C18 column (2.1 × 50 mm, 5 μm) using 5 mM ammonium formate in water (A) and acetonitrile (B) as mobile phase. A linear gradient elution at a flow rate of 0.25 ml/min with total run time of 4 min was as follows: 60% A (0–0.8 min), 10% A (2.0–4.0 min), and 60% A (5.0–6.0 min). TA and budesonide (internal standard) were analyzed in positive ionization mode with following multiple reaction monitoring (MRM) transitions: 435 → 415 (TA); 431 → 413 (budesonide).

2.12. Data analysis

The data obtained for VEGF secretion were fit to sigmoidal inhibitory models with a baseline effect using WinNonlin software (version 1.5; Scientific Consulting, Inc., Cary, NC). Statistical comparisons between two experimental groups were performed using independent samples Student's *t*-test. The results were considered statistically significant at $P < 0.05$.

3. Results

3.1. Preparation and characterization of nanoparticles and microparticles

Triamcinolone acetonide loading was 29.5 and 14.7% for microparticles and nanoparticles, respectively. Nile red content was 0.33 and 0.41% and for microparticles and nanoparticles, respectively. The particle size for nanoparticles and microparticles was 551 and 2090 nm, respectively. Scanning electron microscopy (SEM) was used to study surface morphology. SEM images showed that the particles were spherical in shape with small pores on the surface (Fig. 1).

3.2. In vitro drug release

Release of TA from nanoparticles and microparticles was monitored using UV spectrophotometer. The time for complete release of TA from nanoparticles and microparticles was about 45 and 120 days, respectively. Burst release of 6.31 and 4.97% was observed from nanoparticles and microparticles, respectively (Fig. 1).

3.3. Assessment of CNV

CNV development was monitored before laser treatment and 7 days and 14 days after laser treatment with a fundus camera

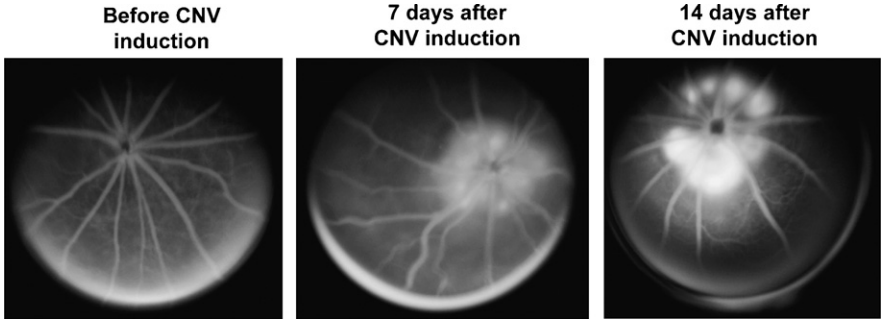

Fig. 2. Development of CNV lesions occurred within 14 days after laser burn in BN rats. Representative fluorescein angiography images assessing CNV induction in Brown Norway rats.

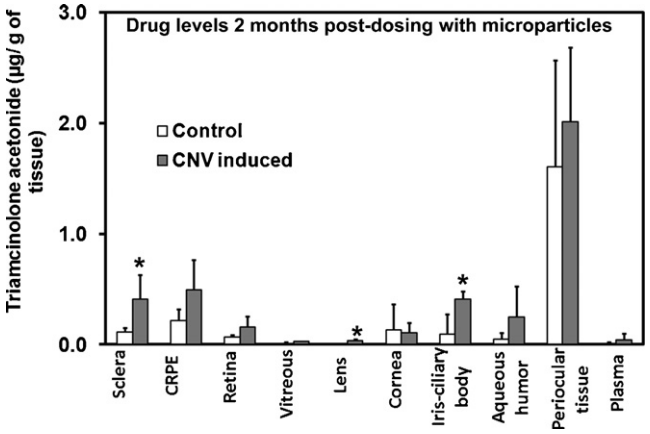

Fig. 3. Single periocular injection of triamcinolone acetonide microparticles sustain the intraocular delivery of TA for 2 months. Tissue distribution of TA in BN rat ocular tissues at the end of 2 months after periocular injection of TA microparticles at a dose equivalent to 150 μg of TA/animal. TA levels in ocular tissues were below the limit of detection (2.5 ng/ml) for the nanoparticle and plain drug suspension groups. Data represents mean ± SD for $N = 4$. * Significantly different from control at $P \leq 0.05$.

(Fig. 2). Sodium fluorescein leakage was seen to increase with time. In comparison to day 7, fluorescein leakage was more at day 14.

3.4. In vivo drug delivery

In vivo delivery of TA was assessed in control and CNV induced BN rats after subconjunctival injection of nanoparticle or microparticle dispersion in PBS (pH 7.4) and plain TA suspension in PBS. At the end of 2 months post injection, no drug levels were detected in any ocular tissues for nanoparticles or the plain suspension group. TA microparticles sustained the delivery of TA for 2 months post injection in both control and CNV induced rats. As shown in Fig. 3, TA levels were the highest in periocular tissue (site of injection). For posterior ocular tissues, the rank order of drug distribution was in the order: choroid-RPE ≥ sclera > retina > vitreous. TA levels in CNV induced rats were 3.6-, 2.3-, 2.4-, 2.9-, and 1.3-folds higher in sclera, choroid-RPE, retina, vitreous, and periocular tissue respectively than control rats. Differences were statistically significant only for sclera, lens, and iris-ciliary body. Although the TA delivery to choroid-RPE, retina, and vitreous in CNV induced rats was not significantly different from control rats, the P values were less than 0.12.

Significant amount of entrapped microparticles were observed in the periocular tissues of both control and CNV induced rats at the end of 2 months post injection. Microscopic visualization of periocular tissues using scanning electron microscope (SEM) and confocal microscope showed the presence of microparticles in periocular tissues (Figs. 4 and 5). Microparticles loaded with Nile red as a tracer dye were visible in red color in confocal microscopy images (Fig. 5).

3.5. Inhibition of VEGF secretion

Triamcinolone acetonide inhibited VEGF secretion from ARPE-19 cells with an IC_{50} of 0.07 ± 0.01 μM. Drug effects were evident at concentrations as low as 0.05 μM (Fig. 6), with the reduction in VEGF secretion being 33%.

4. Discussion

This study, for the first time, shows that the transscleral delivery of TA to the intraocular tissues was higher in CNV induced rats when compared to control animals. Further, we have successfully developed biodegradable polymeric microparticles of TA,

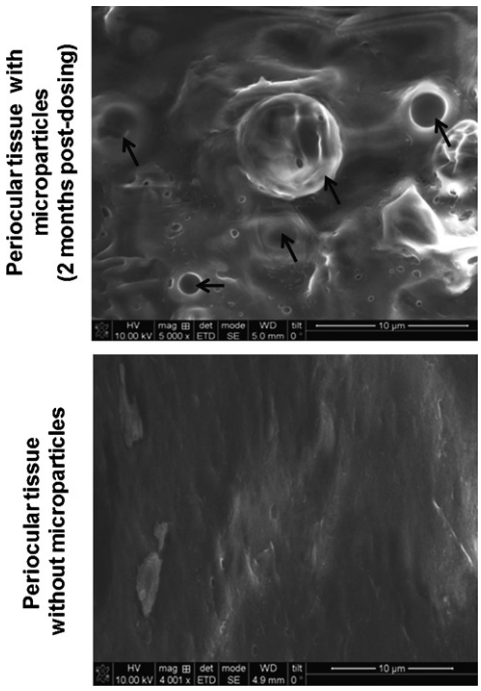

Fig. 4. Assessment of entrapped microparticles in periocular tissues (site of injection) in BN rats 2 months post injection. Pictures were obtained using a scanning electron microscope (JEOL) at 5000× magnification. Arrowhead shows the entrapped microparticles in periocular tissue of BN rats.

which sustained choroidal and retinal delivery for 2 months in therapeutically effective concentration after a single periocular injection. Further, we showed that significant amount of microparticles remain in the periocular space at the end of two months and maintain their spherical shape.

To sustain the long term delivery of TA, polymeric nano- and micro-particles were prepared using poly(L-lactide). Pure poly(L-lactide), has degradation half-life of 12–16 months (Yeo and Park, 2004). Further, TA is a lipophilic drug molecule and entrapment efficiency of lipophilic drugs is much better in a hydrophobic homopolymer such as PLA than a more hydrophilic copolymer such as PLGA. Herein, we demonstrated that particles made with PLA have 14.7% drug loading in nanoparticles and 29.5% drug loading in microparticles (Table 1). Microparticles have better drug loading and entrapment efficiency than nanoparticles since they have lower surface-to-volume ratio, which minimizes surface drug that is removed during particle washes (Lecaroz et al., 2006; Mohanraj and Chen, 2006). For microparticles, entrapment efficiency was 88.5%, whereas for nanoparticles the entrapment efficiency was 44.1%, which is significantly lower than microparticles (Table 1). Surface morphology of particles showed uniform spherical shapes with small pores on the particle surface. Removal of organic solvent from the particle core results in the formation of honeycomb like internal structure and pores on the surface of particles (Yeo and Park, 2004). In vitro release profile showed that microparticles sustained the drug release for longer duration than nanoparticles (Fig. 1). Since nanoparticles are smaller in diameter, their surface area is larger than their volume and hence, the large amount of drug closer to the particle surface results in rapid drug release (Mohanraj and Chen, 2006; Redhead et al., 2001). Previously, we have also shown that in vitro release of budesonide was faster from PLA nanoparticles than microparticles (Kompella et al., 2003). Although we did not measure the residual dichloromethane content in this study, an earlier study of ours employing similar methods indicated that PLA microparticles have a dichloromethane content of about 1 ppb (Shelke et al., 2011).

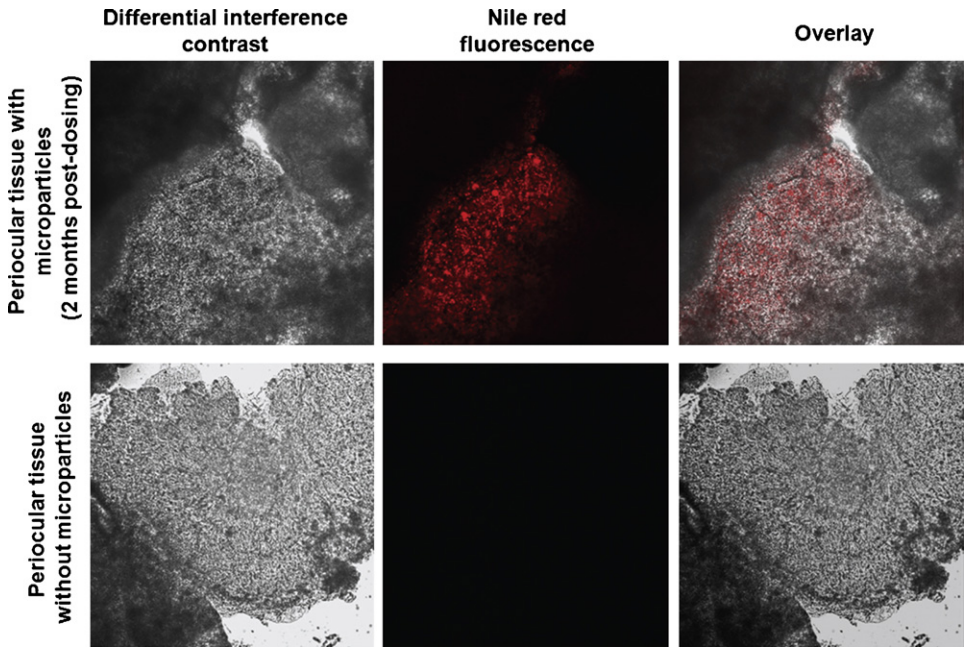

Fig. 5. Confocal microscopy images of periocular tissue were obtained from control and microparticles injected rats. Pictures were obtained using confocal microscope (Nikon C1 si®) set at 20× magnification. Nile red was added as tracer dye in microparticles, which appears red under the microscope. (For interpretation of the references to color in this figure legend, the reader is referred to the web version of the article.)

Table 1
Physicochemical characterization of triamcinolone acetonide loaded poly-L-lactide nanoparticles and microparticles.

Batch	Particle size (nm)	Polydispersity index	Nile red loading (%, w/w)	Triamcinolone acetonide loading (%, w/w)	Triamcinolone acetonide encapsulation efficiency (%, w/w)
Microparticles	2090 ± 302.7	0.043 ± 0.030	0.33 ± 0.027	29.5 ± 2.82	88.5 ± 6.10
Nanoparticles	551.4 ± 80.8	0.146 ± 0.013	0.41 ± 0.038	14.7 ± 1.95	44.1 ± 5.70

Long term sustained in vivo delivery of TA form polymeric particles was evaluated in BN rats after periocular injection. Previously, we showed that budesonide loaded microparticles sustain the choroidal and retinal delivery for 2 weeks whereas, nanoparticles exhibited detectable drug levels for only 7 days after periocular injections in rats (Kompella et al., 2003). The objective of the current study was to sustain TA delivery for at least 2 months after periocular injection. Herein, we demonstrated that single periocular injection of TA microparticles sustained the posterior segment drug delivery for at least 2 months (Fig. 3), whereas no drug levels were detected for plain drug suspension and nanoparticles. Our in vivo results were in agreement with the in vitro release profile of TA from nano- and micro-particles, where nearly 100% of the drug was released within 45 days for nanoparticles and 120 days for microparticles (Fig. 1). Further, a significant amount of microparticles remained at the site of injection even after 2 months, which is expected to sustain the TA delivery for longer periods. Microscopic examination of periocular tissue showed that particles still maintained their spherical shape and were entrapped in the tissue matrix (Figs. 4 and 5). Previously we have shown that PLA microparticles remain in the rabbit vitreous for 3 months after intravitreal injection and maintain its spherical shape and sustain the delivery of hydrophilic drug molecule (Shelke et al., 2011).

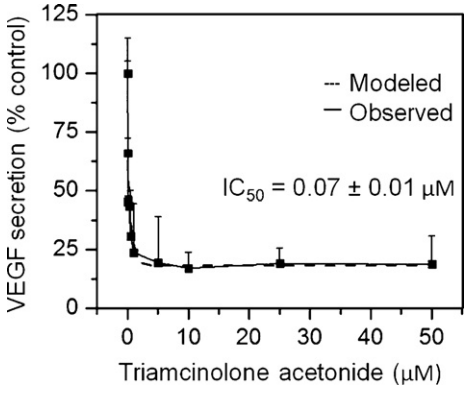

Fig. 6. Triamcinolone acetonide inhibits the VEGF secretion in ARPE-19 cells. Data represents mean ± SD for $N = 6$. The IC_{50} values were calculated using the inhibitory sigmoid E_{max} model with baseline effects.

After subconjunctival injection of TA microparticles, significant amount of drug remained at the site of injection (periocular tissue). Delivery of TA to posterior ocular tissues was in order of choroid-RPE ≥ sclera > retina > vitreous (Fig. 3). TA levels in choroid-RPE were slightly higher than sclera; even though choroid-RPE comes after sclera for subconjunctival delivery. TA is a lipophilic corticosteroid; significant amount of lipophilic drug molecules preferentially accumulate in choroid-RPE due to melanin binding (Thakur et al., 2010). Previously, with subconjunctival injection of corticosteroids and beta-blockers, we observed similar trends of drug distribution to the posterior ocular tissues, with drug levels being higher in choroid-RPE than sclera, retina, and vitreous for lipophilic drugs such as TA (Kadam and Kompella, 2010; Thakur et al., 2010). Significant amount of TA levels were detected in the

anterior segment ocular tissues including cornea, aqueous humor and iris-ciliary body. Delivery of drug to the anterior tissue after periocular injection can be partially explained by leak-back of drug through the needle track as well as diffusion across conjunctiva into the tear film (Cheruvu et al., 2008).

Another objective of the current study was to evaluate the effect of disease state on intraocular delivery of TA after periocular injection. Previously with a diabetic retinopathy model, we showed that the retinal delivery of celecoxib was 2.0-fold higher in diabetic rats than in control rats (Cheruvu et al., 2009). In the current study, there was more TA delivered to all ocular tissues in the CNV induced rats compared to control rats (Fig. 3). Further, the drug levels in the CNV group at the dosing site were 1.3-fold higher but not significantly different from the control group. One possible reason for the increase in TA delivery in CNV induced rats may be due to compromised ocular barriers and altered delivery or clearance in the choroid-RPE and retina. Various literature reports showed that there is a significant reduction in choroidal blood flow in AMD patients compared to normal healthy subjects (Grunwald et al., 1998, 2005). Further, during CNV progression, migration of choroidal endothelial cells in RPE results in disruption of the RPE barrier (Dong et al., 2011; Hartnett et al., 2003), which might increase retinal drug delivery from the periocular site. The combination of reduced blood flow and disruption of ocular barriers may result in higher intraocular delivery of TA in CNV induced rats compared to control rats. Although the TA delivery was higher in CNV induced rats than the control rats, significant differences were only observed with sclera, lens, and iris-ciliary body.

To develop the exposure-response relationship between TA delivery to the choroid-RPE and an efficacy parameter related to CNV, we measured the inhibitory effect of TA on VEGF secretion. An elevation in VEGF levels is a key contributor for the development of ocular neovascular diseases such as CNV and diabetic retinopathy (Miller, 1997). Various studies indicated a central role for elevated VEGF in the pathogenesis of CNV (Spilsbury et al., 2000; Kwak et al., 2000), and it was previously shown that inhibitory effect of TA on choroidal neovascularization can be explained in part by a reduction in VEGF secretion (Tong et al., 2006). Our in vitro VEGF secretion assay in ARPE-19 cells showed a very potent inhibitory effect of TA with an IC_{50} of 0.07 ± 0.01 μM. This effect is in good agreement with previous published reports. Budesonide and fluocinolone acetonide, other potent corticosteroids showed 43 and 37% inhibition of VEGF secretion, respectively, in ARPE-19 cells at 0.1 μM (Ayalasomayajula et al., 2009; Kompella et al., 2003). In our in vivo delivery study, at the end of 2 months, drug levels in the choroid-RPE were 1.14 and 0.48 μM and 0.36 and 0.14 μM in the retina, in CNV and normal rats, respectively. Compared to the IC_{50} for VEGF inhibition, these levels were 16- and 7-fold higher in choroid-RPE and 5- and 2-fold higher in retina of CNV and normal rats, respectively. Thus, single periocular injection of TA microparticles can sustain choroid-RPE and retinal drug levels for at least 2 months at therapeutically effective concentrations.

5. Conclusion

In summary, PLA microparticles are better than nanoparticles in sustaining posterior segment delivery of TA after periocular injection. Spherical microparticles remained entrapped in the tissue matrix at the site of injection after 2 months. Delivery of TA is significantly higher in CNV induced rats than control rats, and polymeric microparticles maintain therapeutic concentrations of TA in choroid-RPE and retina for at least 2 months after a single periocular injection.

Acknowledgements

This work was supported by NIH grants EY017045 (through Emory University), EY018940, and EY017533.

References

Amrite, A.C., Ayalasomayajula, S.P., Cheruvu, N.P., Kompella, U.B., 2006. Single periocular injection of celecoxib-PLGA microparticles inhibits diabetes-induced elevations in retinal PGE2, VEGF, and vascular leakage. Invest. Ophthalmol. Vis. Sci. 47, 1149–1160.

Ayalasomayajula, S.P., Ashton, P., Kompella, U.B., 2009. Fluocinolone inhibits VEGF expression via glucocorticoid receptor in human retinal pigment epithelial (ARPE-19) cells and TNF-alpha-induced angiogenesis in chick chorioallantoic membrane (CAM). J. Ocul. Pharmacol. Ther. 25, 97–103.

Cheruvu, N.P., Amrite, A.C., Kompella, U.B., 2008. Effect of eye pigmentation on transscleral drug delivery. Invest. Ophthalmol. Vis. Sci. 49, 333–341.

Cheruvu, N.P., Amrite, A.C., Kompella, U.B., 2009. Effect of diabetes on transscleral delivery of celecoxib. Pharm. Res. 26, 404–414.

Chin, H.S., Park, T.S., Moon, Y.S., Oh, J.H., 2005. Difference in clearance of intravitreal triamcinolone acetonide between vitrectomized and nonvitrectomized eyes. Retina 25, 556–560.

Dobi, E.T., Puliafito, C.A., Destro, M., 1989. A new model of experimental choroidal neovascularization in the rat. Arch. Ophthalmol. 107, 264–269.

Dong, X., Wang, Y.S., Dou, G.R., Hou, H.Y., Shi, Y.Y., Zhang, R., Ma, K., Wu, L., Yao, L.B., Cai, Y., Zhang, J., 2011. Influence of Dll4 via HIF-1alpha-VEGF signaling on the angiogenesis of choroidal neovascularization under hypoxic conditions. PLoS One 6, e18481.

Grunwald, J.E., Hariprasad, S.M., DuPont, J., Maguire, M.G., Fine, S.L., Brucker, A.J., Maguire, A.M., Ho, A.C., 1998. Foveolar choroidal blood flow in age-related macular degeneration. Invest. Ophthalmol. Vis. Sci. 39, 385–390.

Grunwald, J.E., Metelitsina, T.I., Dupont, J.C., Ying, G.S., Maguire, M.G., 2005. Reduced foveolar choroidal blood flow in eyes with increasing AMD severity. Invest. Ophthalmol. Vis. Sci. 46, 1033–1038.

Hartnett, M.E., Lappas, A., Darland, D., McColm, J.R., Lovejoy, S., D'Amore, P.A., 2003. Retinal pigment epithelium and endothelial cell interaction causes retinal pigment epithelial barrier dysfunction via a soluble VEGF-dependent mechanism. Exp. Eye Res. 77, 593–599.

Jager, R.D., Mieler, W.F., Miller, J.W., 2008. Age-related macular degeneration. N. Engl. J. Med. 358, 2606–2617.

Jonas, J.B., Kreissig, I., Degenring, R., 2002. Repeated intravitreal injections of triamcinolone acetonide as treatment of progressive exudative age-related macular degeneration. Graefes Arch. Clin. Exp. Ophthalmol. 240, 873–874.

Kadam, R.S., Kompella, U.B., 2010. Influence of lipophilicity on drug partitioning into sclera, choroid-retinal pigment epithelium, retina, trabecular meshwork, and optic nerve. J. Pharmacol. Exp. Ther. 332, 1107–1120.

Kompella, U.B., Bandi, N., Ayalasomayajula, S.P., 2003. Subconjunctival nano- and microparticles sustain retinal delivery of budesonide, a corticosteroid capable of inhibiting VEGF expression. Invest. Ophthalmol. Vis. Sci. 44, 1192–1201.

Kompella, U.B., Kadam, R.S., Lee, V.H., 2010. Recent advances in ophthalmic drug delivery. Ther. Deliv. 1, 435–456.

Kwak, N., Okamoto, N., Wood, J.M., Campochiaro, P.A., 2000. VEGF is major stimulator in model of choroidal neovascularization. Invest. Ophthalmol. Vis. Sci. 41, 3158–3164.

Lecaroz, C., Gamazo, C., Renedo, M.J., Blanco-Prieto, M.J., 2006. Biodegradable micro- and nanoparticles as long-term delivery vehicles for gentamicin. J. Microencapsul. 23, 782–792.

Miller, J.W., 1997. Vascular endothelial growth factor and ocular neovascularization. Am. J. Pathol. 151, 13–23.

Mohanraj, V.J., Chen, Y., 2006. Nanoparticles – a review. Trop. J. Pharm. Res. 5, 561–573.

Nowak, J.Z., 2006. Age-related macular degeneration (AMD): pathogenesis and therapy. Pharmacol. Rep. 58, 353–363.

Nowak, J.Z., Bienias, W., 2007. Age-related macular degeneration (AMD): etiopathogenesis and therapeutic strategies. Postepy. Hig. Med. Dosw. (Online) 61, 83–94.

Ozkiris, A., Erkilic, K., 2005. Complications of intravitreal injection of triamcinolone acetonide. Can. J. Ophthalmol. 40, 63–68.

Raghava, S., Hammond, M., Kompella, U.B., 2004. Periocular routes for retinal drug delivery. Expert. Opin. Drug Deliv. 1, 99–114.

Redhead, H.M., Davis, S.S., Illum, L., 2001. Drug delivery in poly(lactide-co-glycolide) nanoparticles surface modified with poloxamer 407 and poloxamine 908: in vitro characterisation and in vivo evaluation. J. Control. Release 70, 353–363.

Robinson, M.R., Lee, S.S., Kim, H., Kim, S., Lutz, R.J., Galban, C., Bungay, P.M., Yuan, P., Wang, N.S., Kim, J., Csaky, K.G., 2006. A rabbit model for assessing the ocular barriers to the transscleral delivery of triamcinolone acetonide. Exp. Eye Res. 82, 479–487.

Schlichtenbrede, F.C., Mittmann, W., Rensch, F., Vom Hagen, F., Jonas, J.B., Euler, T., 2009. Toxicity assessment of intravitreal triamcinolone and bevacizumab in a retinal explant mouse model using two-photon microscopy. Invest. Ophthalmol. Vis. Sci. 50, 5880–5887.

Shah, C.P., Garg, S.J., Vander, J.F., Brown, G.C., Kaiser, R.S., Haller, J.A., 2011. Outcomes and risk factors associated with endophthalmitis after intravitreal injection of anti-vascular endothelial growth factor agents. Ophthalmology 118, 2028–2034.

Shelke, N., Kadam, R., Tyagi, P., Rao, V., Kompella, U., 2011. Intravitreal poly(L-lactide) microparticles sustain retinal and choroidal delivery of TG-0054, a hydrophilic drug intended for neovascular diseases. Drug Deliv. Trans. Res. 1, 76–90.

Spilsbury, K., Garrett, K.L., Shen, W.Y., Constable, I.J., Rakoczy, P.E., 2000. Overexpression of vascular endothelial growth factor (VEGF) in the retinal pigment epithelium leads to the development of choroidal neovascularization. Am. J. Pathol. 157, 135–144.

Sunkara, G., Kompella, U.B., 2003. Membrane transport processes in the eye. In: Ophthalmic drug Delivery Systems. Marcel Dekker Inc., New York.

Thakur, A., Kadam, R.S., Kompella, U.B., 2010. Influence of drug solubility and lipophilicity on transscleral retinal delivery of six corticosteroids. Drug Metab. Dispos. 39, 771–781.

Tong, J.P., Lam, D.S., Chan, W.M., Choy, K.W., Chan, K.P., Pang, C.P., 2006. Effects of triamcinolone on the expression of VEGF and PEDF in human retinal pigment epithelial and human umbilical vein endothelial cells. Mol. Vis. 12, 1490–1495.

Yeo, Y., Park, K., 2004. Control of encapsulation efficiency and initial burst in polymeric microparticle systems. Arch. Pharm. Res. 27, 1–12.